DIRAC Note 2003-01

Systematic Errors in the DIRAC Experiment

Document used for the additional justification of the DIRAC beam time Request CERN/SPSC 2002-034
(SPSC/CERN 2003-005)

A. Benelli, D. Goldin, C. Santamarina, Ch. P. Schütz, L. Tauscher and S. Vlachos for the DIRAC collaboration.

Contents

1 Introduction

The DIRAC experiment aims at measuring with high accuracy the life time of the $\pi^+\pi^-$ atom ($A_{2\pi}$). The lifetime is directly connected to the magnitude of the difference of the scattering lengths $|a_2 - a_0|$. This difference is a key quantity for testing any theory on soft QCD (e.g. chiral perturbation, Lattice etc.).

In the DIRAC experiment $A_{2\pi}$ atoms are produced in collisions of 24 GeV protons with a target nucleus, with a branching fraction of 10^{-9} and accompanied by other secondary particles. Once produced the atoms annihilate or interact with the target material.

The DIRAC method (cf. ref. [1]) of measuring the life time of the $A_{2\pi}$ atoms is based on detecting π^+-π^- pairs from ionized atoms. The break-up probability is linked to the target material and thickness and can be calculated. The survival time until break-up is then linked to the lifetime of the atom.

The π^+-π^- pair of a dissociated atom is characterized by the kinematics (almost equal momenta, very low Q). This pion pair is detected by the high resolution DIRAC double arm spectrometer. The primordial aim of the DIRAC experiment is to find, as a signal of produced atoms, a clear enhancement of low Q track pairs as compared to phase space distributed pairs.

The π^+-π^- background from phase space pions is distorted kinematically for low Q due to Coulomb interaction between the oppositely charged pions. This leads to an enhancement of low Q track pairs with respect to pure phase space (Coulomb correlated (CC) background). The amount of atomic pairs is uniquely linked to the amount of CC background.

Pions from decay of long-lived mesons do not contribute to CC-background, but produce a non-Coulomb enhanced background (NC).

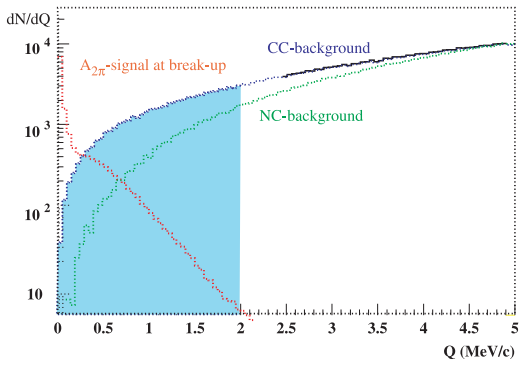

Figure 1: *Relative momentum of the $\pi^+\pi^-$ pairs from atoms after break-up and backgrounds at production. One thousand CC events in the area up to 2 MeV/c (light blue area) correspond to 615 produced atoms. Events generated in the Q-interval from 0 to 7 MeV/c: 15000 atomic pairs, 10^6 CC background, of which 61000 with $Q \leq 2MeV$ and 10^6 NC background.*

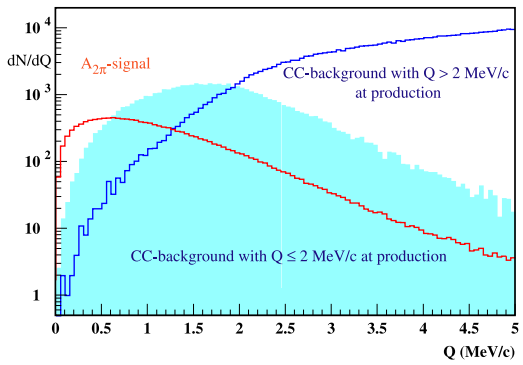

Figure 2: *Relative momenta after the target ($98\mu m$ Ni). The area of CC events with $Q \leq 2MeV/c$ at production is extending up to $Q \geq 5MeV/c$ (light blue area). The background originally above $Q = 2MeV/c$ extends now down to $Q = 0$. The same events are used as for fig.1. For simplicity the NC background is not displayed.*

In extracting the number of atomic π^+-π^- pairs the CC background has to be reconstructed from phase space distributed background. The Coulomb correlation as a function of Q is obtained from theory. Experimentally the phase space distributed background is obtained from accidental background. After correcting the low Q pairs found, the number of surviving atoms can be extracted.

The life time is then obtained from theoretical calculations, which relate the break-up probability to the life time for each target. Break-up is more probable for heavy nuclei than for light ones.

It should be stressed, that the last two steps, Coulomb correlation calculations and break-up probability calculations, are not under the control of the experiment.

2 Signal and Background

An atom which is broken-up produces a π^+-π^- pair (signal). The break-up process (soft Coulomb scattering with target atoms) leaves the longitudinal relative momentum Q_l almost unchanged, but gives a transverse kick to the pions of up to $|Q_T| \approx 4MeV/c$. The Q distribution is shown in fig. 1. Below this sharp atomic signal we have a NC background, which rises like Q^2, and a CC background, which rises like the NC background, but enhanced by the Coulomb correlation function $A_{CC}(Q)$ (see fig. 1) :

$$\begin{aligned} \mathrm{NC-background:} \quad & F_{NC} \propto Q^2 \\ \mathrm{CC-background:} \quad & F_{CC} \propto F_{NC} \times A_{CC}(Q) \ \text{ with } \ A_{CC}(Q) = \frac{\frac{2\pi\alpha m_{\pi^\pm}}{Q}}{1-exp(-\frac{2\pi\alpha m_{\pi^\pm}}{Q})}; \end{aligned} \tag{1}$$

Due to the finite target thickness the sharp atomic pair signal gets smeared by multiple scattering. The corresponding signal and the backgrounds are shown in fig. 2. The integral from Q = 0 to 2 MeV/c of the CC background, which is used for obtaining the number of produced atomic pairs, extends now over a Q-range up to 5 MeV/c or more. The signal extends to up to more than $Q = 5MeV/c$. The backgrounds which originally are above $Q = 2MeV/c$ contribute now events with Q down to zero.

Conclusion: The multiple scattering is deteriorating the signal. The deteriorations concern essentially the transverse plane [1]. The influences of multiple scattering on the signal and backgrounds can only be assessed by MonteCarlo methods. The consequences are:

- Any cut in Q done for optimizing the signal-to-background requires very precise knowledge of the multiple scattering. Else the number of produced atoms deduced from the CC background will have a large systematic error. Thus, a cut of $Q \leq 2MeV/c$, as usually done in DIRAC, implies, that 0.615 atoms were produced

[1] multiple scattering does not affect the magnitude of the momenta.

and that almost all of the atomic pair signal was detected for the case of no multiple scattering (cf. fig. 1). The ratio $\frac{\mathrm{number-of-produced-atoms}}{\mathrm{number-of-CC-events-with}\, Q \leq 2MeV/c}$ for this case is 0.615. The same cut applied for the case with multiple scattering in the target (cf. fig. 2) implies a loss in atomic pair signal of 14% and a loss of CC events with $Q \leq 2MeV/c$ of 40%. The total CC background with $Q \leq 2MeV/c$ thus contains 60% of the CC events with $Q \leq 2MeV/c$ and 40% of CC background from higher Q. Altogether the above ratio (cf. chapter 4.6 and eq. 6) becomes 0.645, while a cut at $Q \leq 2.5MeV/c$ would produce a ratio of 0.416. A systematic 5% increase in the scattering angle results in an increase of the K-factor of 2.5%. **Thus we expect multiple scattering to be a major source of systematic errors.**

- Q_T has to be measured accurately in order to recover the signal. It should be emphasized that the atomic pair signal, which peaks at $Q \approx 1MeV/c$ (cf. fig.2), produces track pairs with a most probable opening angle of 0.5 mrad, i.e. at a distance of two meters from the target the tracks are separated by only about 1 mm. This requires precise tracking with high double track resolution.

3 The Experimental set-up

3.1 The proton beam

The experiment uses the extracted proton beam T8 in the East hall of CERN, which normally provides more than 10^{11} protons per 0.4 sec long spills, at a momentum of 24 GeV/c.

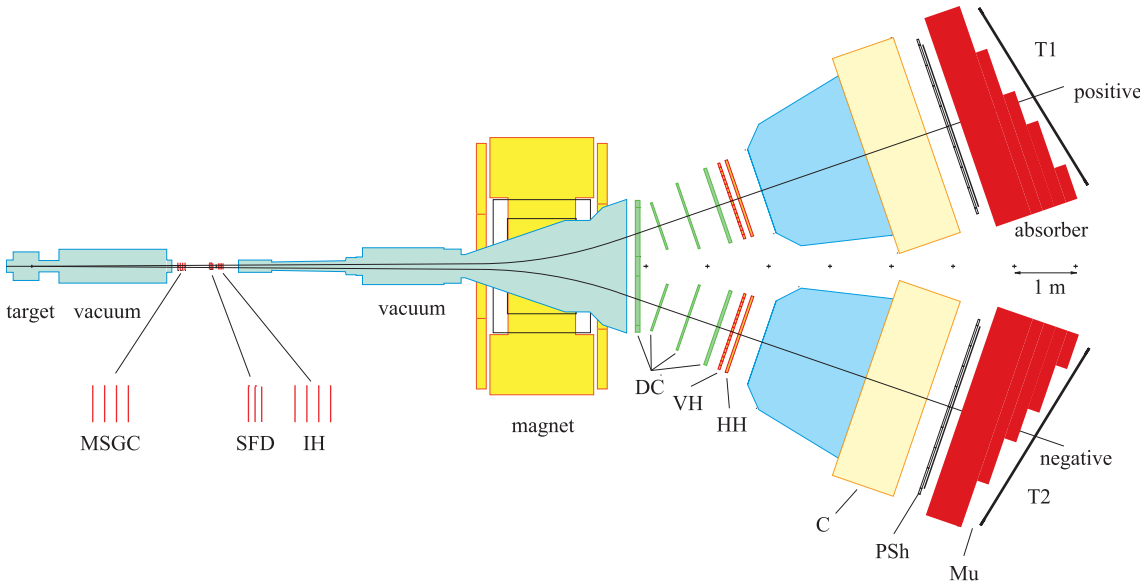

Figure 3: *Top view of the DIRAC spectrometer. Upstream detectors: four Micro Strip Gas Chambers (MSGCs), two Scintillation Fiber Detectors (SFD), Ionisation hodoscopes (IH). Downstream of the magnet, for each arm: four sets of drift chambers (DC), one vertical (VH) and one horizontal (HH) hodoscope, one Cherenkov counter (C), one preshower (PrSh), and, after the absorber, one muon counter (Mu).*

3.2 The Apparatus

A schematic view of the apparatus is shown in Figure 3. The proton beam hits the target (typically 100 to 300 μm thick foils) and continues to the beam dump. The *double arm spectrometer* spans a plane inclined upwards with respect to the horizontal by 5.7^o and has an opening angle of $\pm 1.0^o$ horizontally and vertically with respect to the target. The *magnet* has a bending power of 2.2 Tm. 2.3 meters downstream from the target the secondary particles pass through a set of *coordinate detectors* ($10 \times 10cm^2$). The target and the drift region up to the *coordinate detectors* is in vacuum. After the coordinate counters the particles enter a vacuum vessel, pass through a collimator and enter the magnet. After the magnet the vacuum ends. The *arms of the spectrometer* are symmetric, $\pm 19^o$ with respect to no deflection.
The *coordinate detectors* consist of

- four layers of single GEM MSGCs with a typical efficiency of 92% per layer, and double track resolution of 0.4 mm. These chambers are used for upstream tracking.
- one layer of vertical and one horizontal scintillation fibers (SFD). Since spring 2002 a third (U) layer is operational. These detectors are the main instruments for upstream tracking.
- two layers of vertical plastic scintillator hodoscopes (subsequently called IH), consisting of 16 counters each. Since June 2001 a new hodoscope is in place, consisting of two staggered layers of vertical and two staggered layers of horizontal hodoscopes. These detectors are used to resolve ambiguities when two tracks are too close together and not resolved by the upstream tracking.

Each *arm of the spectrometer* is equipped with

- four sets of drift chambers, each containing 14 coordinate planes.
- one vertical hodoscope, read-out on both ends for good timing (henceforth called VH)
- one layer of horizontal scintillator hodoscopes (HH), read out on both sides
- a threshold gas Cherenkov counter for electron and positron rejection,
- a (vertical) preshower scintillator hodoscope (PrSh),
- an iron absorber,
- one (since 2000 two) layers of muon counters.

The apparatus is expected to have a relative track pair momentum resolution of $\sigma_Q = 1 MeV/c$.

3.3 Triggers

DIRAC has several *fast triggers* with decision times less than 100 ns:

- $T1$, which requires that IHs had at least one hit and both arms had at least one hit in VHs, HHs and PrSh.
- The "coplanarity" trigger restricts the vertical opening angle between the two tracks through cuts on HH(right)-HH(left).
- Conditions on the signal height in the Cherenkovs allow to define "e^+e^-" or "$\pi^+\pi^-$" pairs.

Since June 2000 DIRAC has also a *minimum bias* trigger, which requires at least one hit in the IHs, and at least one hit in the VHs of the negative arm.
The *2nd level triggers* need $T1$ for being launched.

- DNA (operational since September 1999) uses IHs, VHs and PrSh and selects on neural network algorithms. Decision time 200 ns.
- RNA works analogously to DNA, uses, however, the scintillation fibers instead of the IHs. It has been implemented in July 2001. Decision time 300 ns

The *4th level trigger (T4)* is using the wire information of the four drift chambers. It first verifies, that a track candidate is available per arm and then correlates the two arm track candidates for momentum cuts. The decision time is about 4 μs. T4 is active since June 2001.

3.4 Simulations of the apparatus, the detectors and the triggers

The apparatus (target, vacuum vessels, detector materials including segmentations), the detector responses and detector read-outs as well as the triggers are simulated following closely the used hardware. A GEANT simulation of an event produces exactly the same data structures as does the real experiment.

4 Analysis

The event selection from the raw data is based on unambiguous reconstructibility of a track pair originating from the target. The procedure is as follows:

- first, at least one track per arm is reconstructed as a straight line from the DC and VH information.
- each track is transferred through the magnet and continued as a straight line to the target. This provides a first estimate of the momentum.
- The SFDs are checked for hits close to the intersection of the above tracks with the SFD plane.
- The associated SFD hit is used for a new determination of the momentum.
- In case of neighboring hits, the corresponding IHs are checked for double ionisation.

The procedure looks straight forward, but there are various aspects and features which may lead to biased or even false reconstruction:

- due to multiple scattering the up-stream coordinate detectors altogether produce a kink in the track which leads to a sagitta as large as 1 cm. For small Q (close lying hits) the track-hit assignment may become ambiguous.
- due to multiple scattering in the downstream detectors, especially the first DC-layer and the Al exit window, the downstream tracks may already provide wrong inclinations and thus wrong momenta (x-direction) or wrong hit expectations (y-direction) in the SFD.
- the SFD detector suffers from a small optical leakage to adjacent fibers. In order to suppress more than one hit per track, a signal processor is used, which merges simultaneous signals from adjacent fibers into one signal. However, this leads also to merging of two adjacent real hits from two close lying tracks, as we expect from the atomic pair signature.
- any loss of one hit in the SFD due to efficiency may produce a candidate for a presumed merged hit from two tracks

All these features may lead to systematic errors. In DIRAC we use therefore two methods for reconstruction, the “standard” Dirac method and the “BASEL” method, which are different in some important points. The BASEL studies are largely based on MonteCarlo simulations, using the best detector, trigger and signal processor descriptions. (see ref. [2, 3, 4, 5, 6]).

4.1 SFD hit distributions.

The measured differences of hit locations for prompt (time differences $-0.5ns \leq \Delta t_{VH} \leq 0.5ns$) and accidental (time differences $-16ns \leq \Delta t_{VH} \leq -5ns$) events are shown in fig. 4. The merging of adjacent hits is clearly seen as a 40% dip left and right of a peak at $\Delta SFD = 0$ for prompt events. Events with $\Delta SFD = 0$ correspond to only one available hit for two tracks, and are due to true single hits, merged double hits and lost hits anywhere due to inefficiency. The latter category is reduced in the figure fig. 4 by requiring the corresponding IHs to show double ionisation. Accidental pairs do not show the merging of adjacent hits.

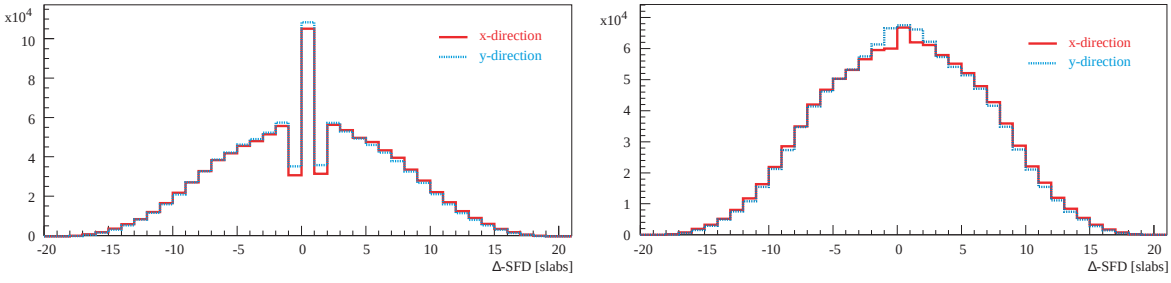

Figure 4: *The difference in SFD hit locations for prompt (left) and accidental (right) events for x- and y- direction, in units of fibers, from all Ni-2001 data. A cut was applied on* $Q_{trans} \leq 4MeV/c$.

4.2 Reconstruction of atomic pairs.

The above difficulties were partly overcome by a number of hit assignment algorithms. Using the simulated atomic pair distributions we have studied the deviations of reconstructed parameters from the input parameters. Fig.5 shows the atomic pair distribution right after the target (hence including the multiple scattering in the target) and the reconstructed distribution. Fig. 6 shows the difference between reconstructed and generated events for Q_x, Q_y and Q_l.

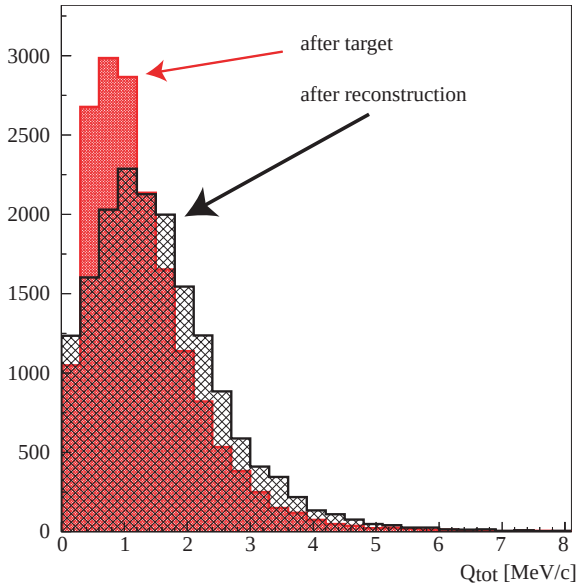

Figure 5: *The atomic pair distributions (right after the target and after reconstruction) as a function of reconstructed Q [MeV/c]*

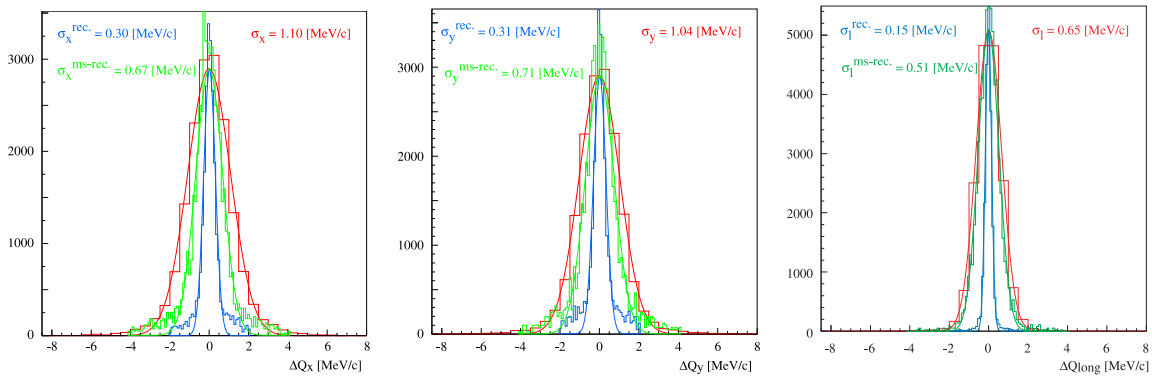

Figure 6: *The difference between input (at production) and reconstruction for Q_x, Q_y and Q_l as a function of reconstructed $Q_{x,y,l}$. For comparison, the differences are also given for multiple scattering in the target only, but no multiple scattering in the apparatus (blue). The difference between Q's after the target and after reconstruction with full multiple scattering in the apparatus are shown in green. The tails are due to wrong hit-track assignments.*

The reconstruction is satisfactory for atomic pairs, the reconstruction efficiency is close to 100%, except for cuts in $Q_{x,y,l}$.

4.3 Accidentals.

The accidental pair distributions do, by definition, not show Coulomb correlations at low Q. Thus they are used to reconstruct the CC background by multiplying the accidental distributions with the Coulomb enhancement function. Two difficulties are encountered:

- the measured accidentals have to be corrected for the different SFD response as compared to prompt ones (cf. fig.4)
- the Coulomb enhancement function as a function of Q, though theoretically well known, has to be obtained for reconstructed distributions.

The BASEL method: The measured accidentals receive their prompt feature by merging with the adequate probability two adjacent SFD hits into one. In this way the accidentals obtain the same SFD characteristics as the prompt events. Fig. 7 shows the corrected accidentals, to be compared with the prompt distribution in fig. 4. This sample is then used for reconstruction.

The "standard" DIRAC method: The "standard" DIRAC method leaves the accidental distributions unchanged and proceeds to reconstruction. The adjustment to the prompt distributions is done afterwards by giving adjacent hit or single hit events the appropriate weight.

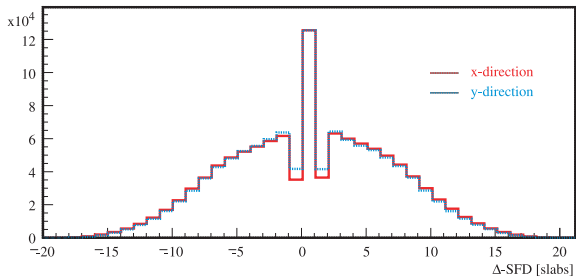

Figure 7: *SFD hit location differences for the corrected accidentals (BASEL method).*

Conclusion: Both methods are fundamentally different. The Basel method transforms the measured accidentals into a data sample which has much the same features as the prompt events and thus no bias is introduced when reconstructing the two. The "standard" DIRAC method reconstructs first the measured accidentals, thus avoiding complications due to SFD response, and applies the SFD induced corrections afterwards. We expect the two methods not to provide identical results.

4.4 Coulomb correlation function.

The Coulomb correlation produces an enhancement of background, which is largest for small Q, hence overlaps with the atomic signal. The correct construction of the "experimental" Coulomb correlation function constitutes the most difficult part in the analysis. The theoretical Coulomb correlation function (cf. equation 1) is modified because of

- multiple scattering in the target,
- apparative inefficiencies,
- reconstruction methods.

While the BASEL method relies on Monte Carlo methods, the "standard"DIRAC method is more analytical and applies a folding of the theoretical Coulomb enhancement function. In any case the "experimental" correlation function is a function of the reconstructed Q_{rec}.

The BASEL method: The pure phase space (NC) distributed events are generated, passed through the target and the detector (GEANT) and reconstructed (*AccR*(Q_{rec}). The CC events were obtained by enhancing the NC events with the Coulomb correlation function and passing them through the simulation in the same way as the NC events (*CcorrR*(Q_{rec}). The NC- and CC-backgrounds are simulated as prompt events. The ratio of $CcorrR/AccR$ provides the "experimental" Coulomb correlation function of Fig. 8. This function, multiplied by the corrected accidental distribution provides the reconstructed Coulomb correlated background ($CC_{rec}(Q_{rec})$.

The "standard"DIRAC method: The reconstruction of a measured accidental event provides an error matrix, which is used to fold the theoretical Coulomb correlation function (A_{CC} with the adequate distributions ($F(Q^{measured}_{x,y,l})$):

$$A_{experimental}(Q^{measured}) = \int A_{CC}(q_{x,y,l}) \times F(Q^{measured}_{x,y,l} - q_{x,y,l}) dq_l dq_x dq_y \qquad (2)$$

The procedure provides as many values for the "experimental" correlation function as there are accidental events. This distribution multiplied by the measured accidental distribution provides the CC background, which then has to be corrected for the different SFD response (cf. chapter 4.3).

Conclusion: The "experimental" Coulomb correlation functions as obtained by the two methods differ largely for $Q \leq 5MeV/c$, while at larger Q the differences to the theoretical Coulomb correlation function are negligible. This discrepancy demonstrates the delicate conspiracy of detector response and reconstruction features in obtaining the "correct" shape of the Coulomb correlation to be applied to the data.

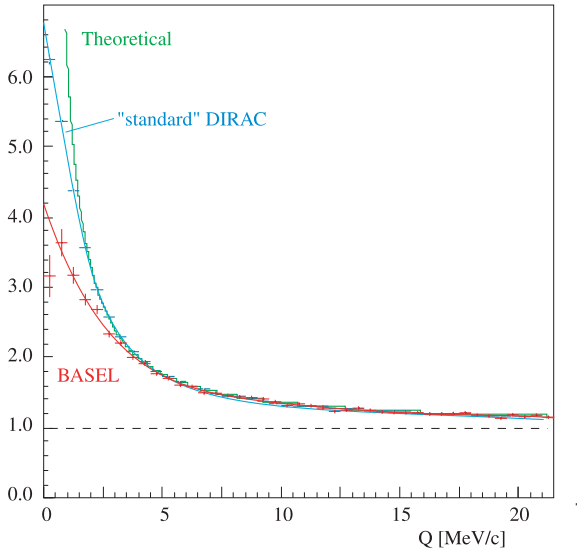

Figure 8: *"Experimental" Coulomb correlation function obtained by the BASEL method (red) and by the "standard" DIRAC method (blue). For comparison the theoretical Coulomb correlation function (green) is also displayed.*

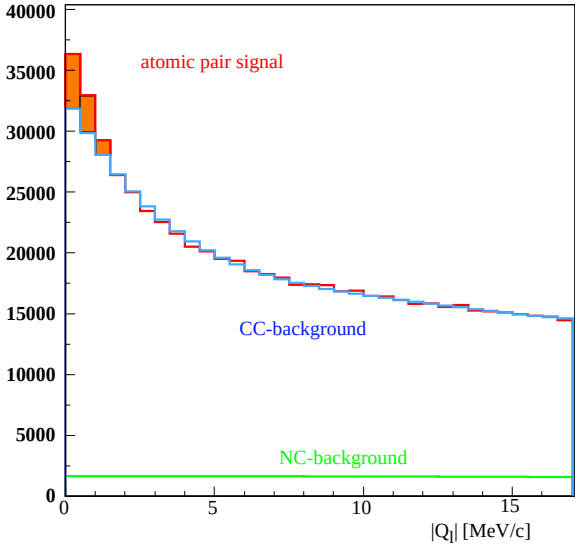

Figure 9: *Q_l fit of CC- (blue) and NC (green) background and of signal (filled red) to the measured Q_l-distribution. Remark the very different shapes of CC- and NC backgrounds, which allow to fit the two without major correlations.*

4.5 Signal extraction

The BASEL and the "standard" DIRAC methods use different approaches to extract the signal.

BASEL signal extraction: The atomic pair signal is obtained from the prompt measured spectrum by fitting the properly parameterized reconstructed CC background (cf. chapter 4.4), the corrected accidental distribution (NC background and accidentals in the prompt window) and the atomic pair signal to the measured prompt distribution. Due to the very different shapes of CC and NC background in Q_l and due to the much lesser sensitivity of the CC background to the low Q_l enhancement, these fits are done in the Q_l distributions (cf. fig. 9).

Fig. 11 shows the signal after the properly fit backgrounds were subtracted in the Q distribution. The signal shape is in remarkable agreement with the simulated prediction for atomic pairs (see fig. 5).

The 'standard" DIRAC signal extraction: The reconstructed CC and NC backgrounds as obtained from the measured accidentals are fitted to the prompt distribution in a region above the signal ($Q > 5MeV/c$). This fixes the heights of the reconstructed CC and NC backgrounds. Subtraction of these backgrounds from the prompt spectrum in the signal region provides the signal.

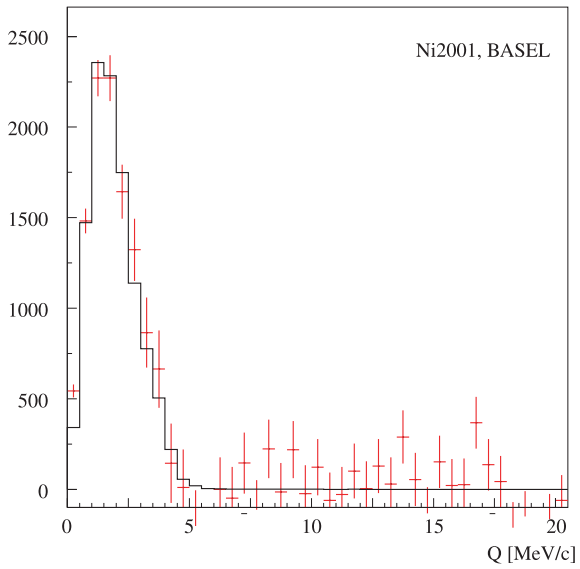

Figure 10: *Atomic pair signal as obtained with the BASEL method from the 2001 Ni data (very preliminary). The solid line is the fitted residual for the signal.*

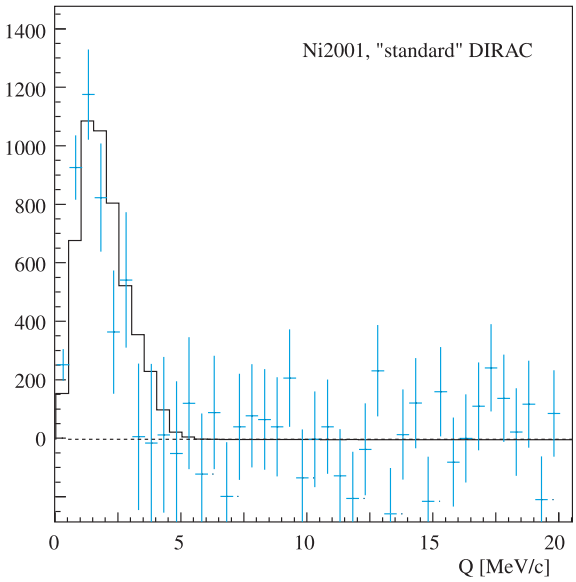

Figure 11: *Atomic pair signal as obtained with the standard DIRAC method from the 2001 Ni data. The solid line represents the signal shape.*

As an example we give approximative results of the two methods for the Ni-2001 data:

$BASEL$	$10000 \pm 400_{stat}$
$standardDIRAC$	$5000 \pm 400_{stat}$

Conclusion: The very different assessment of the CC background (cf. chapter4.4) and the reconstruction of the accidentals leads to a difference in reconstructed signal strength of more than 10 standard deviations.

4.6 The K-factor and Break-up Probability

The K-factor links the number of observable atomic pairs ($N_{signal}^{Q \leq Q_{cut}}$), assuming 100% break-up probability, to the number of observed CC events with $Q \leq Q_{cut}$, $N_{C\bar{C}}^{Q \leq Q_{cut}}$ (see also chapter 2) :

$$N_{signal}^{Q \leq Q_{cut}} = \mathrm{K} \times N_{C\bar{C}}^{Q \leq Q_{cut}} \tag{3}$$

The K-factor does not cause problems if no cuts are applied in Q, Q_x, Q_y or Q_l, because the acceptances of the apparatus for atomic pairs and CC-background with $Q \leq 2MeV/c$ are equal. If, however, cuts are applied, the quality and efficiency of reconstruction have to be known as a function of Q. Moreover, the amount of CC background as compared to the NC and accidental background in the prompt distributions have to be known from the fit with sufficient accuracy.

The procedure is as follows: The number of events having an initial (*init* means *at production*) $q_{init} \leq 2MeV/c$ is linked to the number of reconstructed CC within the cut limits by k:

$$N_{CC}^{q_{init} \leq 2MeV/c} = \mathbf{k} \times N_{C\bar{C}}^{Q \leq Q_{cut}} \tag{4}$$

The factor **k** has to be determined by simulation.

The number of produced atoms thus is:

$$N_{atom} = 0.615 \times \mathbf{k} \times N_{C\bar{C}}^{Q \leq Q_{cut}} \tag{5}$$

Counting the number of atomic signal events within the cut limits provides the signal acceptance (ϵ_{signal}).

The observed atomic pair signal within the cut limits is linked to the number of produced atoms by the break-up probability:

$$P_{br} = \frac{N_{signal}}{\epsilon_{signal}} \times \frac{1}{N_{atom}} = \frac{N_{signal}}{\mathrm{K} \times \sum_{cut-limits} CC(Q_{reconstructed})} \tag{6}$$

with $\mathrm{K} = \epsilon_{signal} \times 0.615 \times \mathbf{k}$.

The BASEL method: The atomic pair signal as well as the CC background are generated according to the theory of break-up and Coulomb enhancement. These events are then simulated with GEANT, including the target, and reconstructed.

The "standard" DIRAC: Same as the BASEL method.

As a result figure 12 shows the signal as well as the CC background after reconstruction (98μm Ni target). Cutting on $Q \leq 2MeV/c$ provides $\epsilon_{signal} = 48\%$, $\frac{N_{CC}^{q_{init} \leq 2MeV/c}}{(N_{CC}^{Q \leq Q_{cut}})} = 1.59$ for $Q_{cut} = 2MeV/c$. This provides a K-factor of K=0.47. Cutting at $Q_{cut} = 2.5MeV/c$ provides a K-factor of K= 0.34.

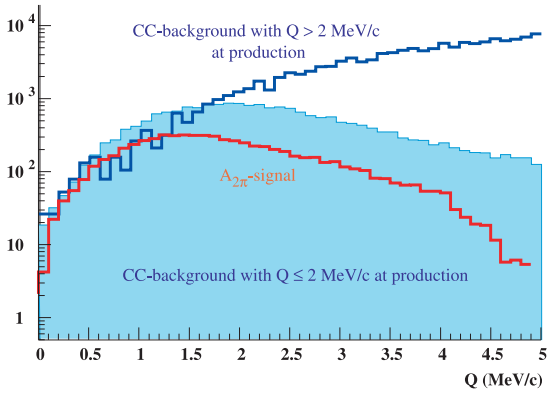

Figure 12: *Reconstructed signal and backgrounds in analogy to fig.2*

Conclusion: Since the observed CC-background increases with increasing Q_{cut} while the signal disappears slowly, the signal shape obtained from reconstruction as well as the CC reconstruction enter directly into the normalisation.

5 Systematic errors.

Summarizing the above the following sources of systematic errors have been identified to be most serious:

- reconstruction of the CC background (cf. chapters 4.3 and 4.4)
- multiple scattering and K-factor (cf. chapters 2 and 4.6)

These errors may be eliminated or reduced by dedicated measurements.

5.1 Measurement of the CC and NC backgrounds with a multi-layer target.

We have studied a measurement on a Ni target, which has the same thickness as our standard target, but is segmented into 12 equally thick layers at distances of 1.0 mm. Compared to the standard target this target has the following properties:

- the production of secondary particles by the beam is identical,
- the integral multiple scattering is the same,
- the amount of atoms produced is the same,
- the amount of atoms which break up is smaller because of enhanced annihilation, i.e. the atomic pair signal is smaller.

By comparing the distributions obtained with such a multi-layer target with the ones of the standard single-layer target allows, with adequate statistics, to determine the signal shape and the prompt background without any manipulations, since all the uncertainties (reconstruction, Monte Carlo etc.) cancel.

5.1.1 Results of the exploratory multi-layer target measurement

We have studied such a multi layer target in an exploratory run in fall 2002. (see also ref. [7]). The results of a 4 weeks run with the multi-layer target are encouraging. We have about 0.6 million events with the multi-layer target and 1.2 million with the single-layer target within the same measuring periods.

Accidentals. First we compare the accidentals of the single-layer and the multi-layer targets. The comparison allows to verify whether the two targets do introduce differences due to their different geometrical dimensions. The ratios single-layer to multi-layer target are shown in the figures 13.

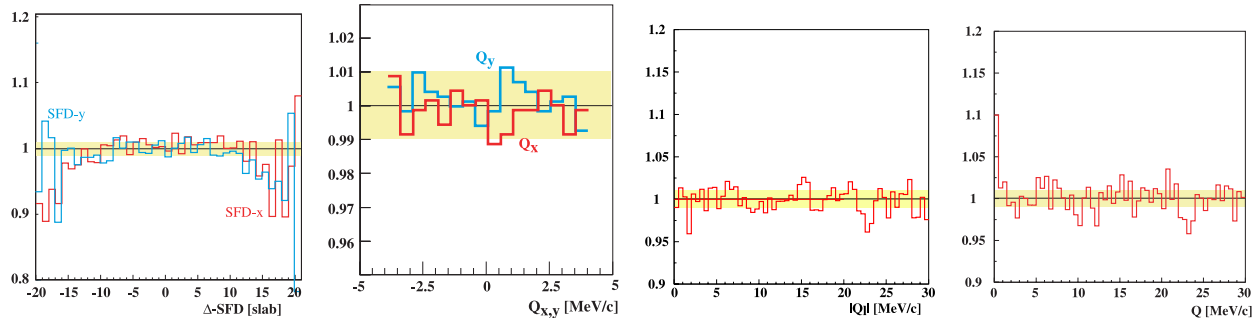

Figure 13: *Ratio of single- to multi-layer target for accidentals, after proper normalisation, for* $\Delta - SFD, Q_{x,y}, Q_l$, *and* Q.

Results: In all relevant distributions for the accidentals the ratios of the single-layer to the multi-layer target scatter around unity within a band of roughly $\pm 1\%$, except for the SFD distributions, where the deviations indicate,that the multi-layer target produces broader patterns. In the reconstructed $Q_{x,y}, Q_l, Q$, however, there is no visible bias. All these features are fully reproduced in the Monte Carlo simulation.

Prompt events: Comparing the real (prompt) events for the single-layer and the multi-layer targets in the same way as was done for the accidentals above we obtain the figures 14. There are biases for SFD similar to the ones for the accidentals. For the reconstructed $Q_{x,y}$ the ratios scatter around unity within a band of $\pm 1\%$. The same is true for Q_l and Q, except for the region below $Q_l, Q = 5 MeV/c$, where the excess signal of atomic pairs in the single-layer target shows up.

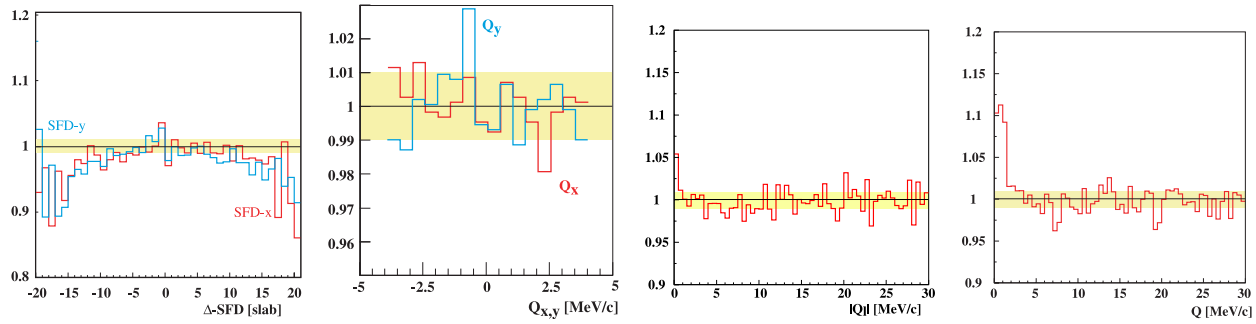

Figure 14: *Ratio of single- to multi-layer target for real (prompt) events, after proper normalisation, for* $\Delta - SFD, Q_{x,y}, Q_l$ *and* Q.

The same exercise may be done for the differences instead of the ratios.

Construction of Background. The number of atoms as well as the backgrounds are the same in single-and multilayer target. The prompt events are thus composed of the backgrounds N_{backgr} and of the atomic pair signal, which is equal to the break-up probability ($P_{br}^{single,multi}$) for the target times the number of atoms produced (N_{atoms}). The difference of multi-layer and single layer target is thus:

$$D(Q) = N^{multi} - N^{single} = (P_{br}^{multi} N_{atoms} + N_{backgr}) - (P_{br}^{single} N_{atoms} + N_{backgr}) \quad (7)$$

The pure background is obtained by minimizing the signal for the Q_l distributions:

$$D(\epsilon, Q_l \leq 0.5) = (\epsilon \times P_{br}^{multi} - P_{br}^{single}) N_{atoms} + (\epsilon - 1) N_{backgr} \quad (8)$$

This is done by evaluating the signals in single- and multi-layer distributions for Q_l (cf. fig. 15) using the MonteCarlo CC and NC background as described in chapter 4.5 for the signal extraction from the Ni2001 data. The signal heights obtained after normalisation are $N_{signal}^{single}(Q_l \leq 0.5) = 1673 \pm 78$ and $N_{signal}^{multi}(Q_l \leq 0.5) = 890 \pm 110$ events. This leads directly to $\epsilon_0 = 1.88 \pm 0.24$ for the difference in the signal to be zero (cf. eq. 8). For ϵ_0 the difference becomes $D(Q) = (\epsilon_0 - 1) N_{backgr}$ and describes the experimentally determined background (cf. fig.16).

The reconstructed background amounts to 6550 ± 172 events up to and including $Q = 2MeV/c$.

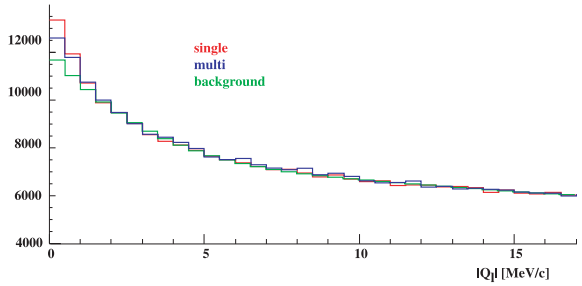

Figure 15: *The Q_l-distributions for single(red), multi (blue) layer targets, and of the background. The difference in signal height at $Q_l = 0$ is clearly visible.*

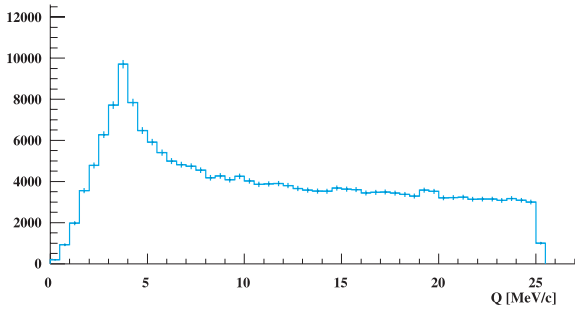

Figure 16: *The residual difference of $\epsilon_0 \times$ multi-layer minus single-layer target as a function of Q, representing the experimentally determined background.*

Conclusion: The background reconstruction using the multi-layer measurements is working well. The result is only weakly depending on the method of background reconstruction. It does not need any further input from theory and can directly be applied to the previously measured data. The accuracy obtained with the exploratory measurement provides a background uncertainty, which is 1.5 times the statistical uncertainty of the atomic pair signal obtained sofar. [2]

References

[1] The DIRAC collaboration, B. Adeva et al., Lifetime measurement of $\pi^+\pi^-$ atoms to test low energy QCD predictions, Proposal, CERN/SPSLC 95–1 (1995).

[2] C. Schuetz and L. Tauscher, "The BASEL SFD Y prediction method in the DIRAC experiment", DIRAC NOTE 02-04

[3] C. Schuetz and L. Tauscher, "The behaviour of the BASEL extended tracking and the standard Ariane tracking to A(2pi) Monte Carlo data in the DIRAC experiment", DIRAC Note 02-01

[4] C. Schuetz, "Detector response simulation for the vertical and horizontal hodoscopes in the DIRAC experiment", DIRAC NOTE 01-07

[5] D. Goldin, L. Tauscher, "Scintillation fiber detector efficiency study", to appear as DIRAC NOTE

[2] The ϵ_0 determination may be used independently to deduce the break-up probability for the Ni-target and from this to obtain the life time without any normalistion or shape complications (K-factor, CC and NC background).

[6] D. Goldin, L. Tauscher, "Scintillating fiber detector background study and simulation", DIRAC NOTE 02-06

[7] C. Santamarina, "A proposal to measure Coulomb background with a multilayer Berylium target", to appear as a DIRAC note

[8] The DIRAC collaboration, B. Adeva et al., "First Observation of πK Atom and its Lifetime Measurement", Addendum to the proposal, CERN/SPSC2000-032, SPSC/P284 Add.1, 17. August 2000